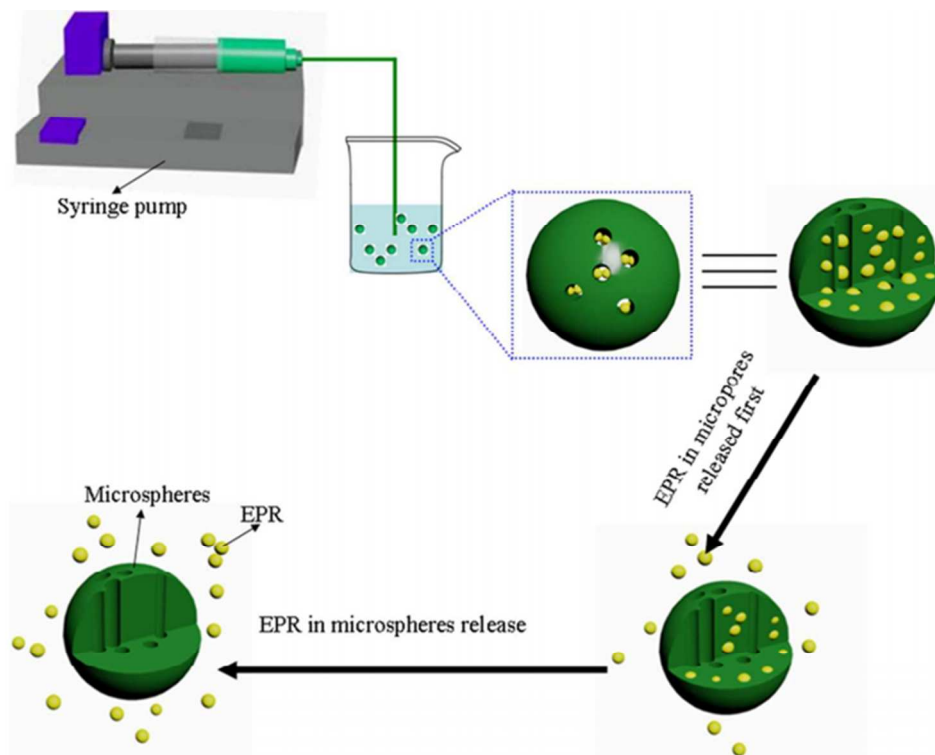




**Fabrication, Characterization, and Controlled Release of  
Eprinomectin from Injectable Mesoporous PLGA  
Microspheres**

Journal:	<i>RSC Advances</i>
Manuscript ID:	RA-ART-06-2015-012262.R1
Article Type:	Paper
Date Submitted by the Author:	18-Aug-2015
Complete List of Authors:	Shang, Qing; Hebei University of Science and Technology, Zhai, Jianhua; Hebei University of Science and Technology, Tian, Ruiqiong; Hebei University of Science and Technology, Zheng, Ting; Zhongqi pharmaceutical technology (SJZ) CO., LTD, Zhang, Xiaoyun; Hebei University of Science and Technology, Liang, Xiaoyang; Hebei University of Science and Technology, Zhang, Jing; 616048475@qq.com,



254x190mm (96 x 96 DPI)

## **Fabrication, Characterization, and Controlled Release of Eprinomectin from Injectable Mesoporous PLGA Microspheres**

**Qing Shang<sup>1,\*</sup>, Jianhua Zhai<sup>1</sup>, Ruiqiong Tian<sup>1</sup>, Ting Zheng<sup>2</sup>, Xiaoyun Zhang<sup>1</sup>,  
Xiaoyang Liang<sup>1</sup>, Jing Zhang<sup>1</sup>**

*<sup>1</sup>Chemical and pharmaceutical engineering institute, Hebei University of Science and  
Technology, 050018 Hebei, China; E-mail: shangqingyl@163.com*

*<sup>2</sup>The institute of pharmaceutical research, Zhongqi pharmaceutical technology (SJZ)  
CO., LTD, 050018 Hebei, China;*

*\*Corresponding author:*

*Address: Chemical and pharmaceutical engineering institute, Hebei University of  
Science and Technology, 050018 Hebei, China;*

*E-mail address: shangqingyl@163.com (Q. Shang).*

*Tel/Fax: +86 0311 81668393.*

**Abstract**

Batches of mesoporous poly(lactide-co-glycolide) (PLGA) microspheres were fabricated *via* an O/W emulsion-solvent evaporation method. The obtained microspheres were detected with an S-4800 scanning electron microscope (SEM) to observe their surface morphology. Observing found that many macropores distributed on microspheres' surfaces. Then, eprinomectin (EPR) was employed as a model drug and encapsulated into these mesoporous microspheres. The distribution states of EPR in microspheres were investigated *via* X-Ray diffraction and differential scanning calorimetry. Test results indicated that EPR distributed in microspheres with an amorphous state. After re-dispersing EPR-loaded microspheres in ultrapure water, an extended-release formulation of EPR was obtained. The formulation was administrated to Japanese white rabbits by subcutaneous injection to monitor the blood concentration of EPR. Plasma concentration profiles showed that the  $C_{max}$  of EPR ( $38.80 \pm 9.50$  ng/mL) was appeared at the 2<sup>nd</sup> day after subcutaneous injection. During the next 40 days, the plasma concentrations of EPR were maintained at 35.0 ng/mL. In addition, the biocompatibility of EPR-loaded mesoporous microspheres (EPM) was also investigated by biological sectioning method. Photographs of histological section illustrated that the EPM did not trigger serious stimulus responses at the injection sites. Thus, it could affirm that the mesoporous microspheres had a promising application in controlling veterinary drug for sustained release.

**Keywords:** DSC; Morphology; Plasma concentration; Drug delivery systems; Veterinary drug

## 1. Introduction

The avermectins, a series of macrocyclic lactone endectocides, are the derivatives of natural fermentation products derived from the genus *Streptomyces*.<sup>[1]</sup> The avermectin families mainly include ivermectin, doramectin, moxidectin, emamectin, and eprinomectin (EPR).<sup>[2-6]</sup> They are extremely effective against (endo-) internal and (ecto-) external parasites even in very low doses. Among the avermectin families, EPR is the first drug licensed for treatment of parasitic infections in lactating cows because of its low residue level in cattle milk.<sup>[7-10]</sup> Besides, EPR has high effects on all stages of major gastrointestinal nematodes, lungworm, lice, horn fly and mange mites of cattle, and has significantly persistent activities for a range of major nematodes.<sup>[11-12]</sup> However, the low water solubility (6.0 - 9.0  $\mu\text{g/L}$ ) of EPR reduces its bioavailability and persistence in oral or injection preparations. Therefore, the main dosage forms of EPR are pour-on solutions.<sup>[13]</sup> The repeated and indiscriminate application has resulted in treatment failures and resistance in some animal species.<sup>[14]</sup> Worse still, the pour-on solutions are difficult to kill the endoparasite of livestock. These shortcomings of pour-on solutions will restrict the application of EPR in certain range.

In recent years, microspheres parenteral delivery systems (MPDS) for controlled drug releasing has aroused researchers' interests.<sup>[15]</sup> MPDS can act as "depot" devices to maximize the drug bioavailability and provide appropriate therapeutic levels throughout treatments.<sup>[16]</sup> These methods increase animal compliance, reduce discomfort, and decrease the fluctuation of plasma concentration.<sup>[17-18]</sup> Owing to

these inherent merits, MPDS have been employed in the fabrication of veterinary drug sustained release formulations.[19] Obviously, this technology can prolong the activity of EPR and maintain its constant persistent effectiveness.

Due to its excellent biocompatibility and biodegradation, PLGA microspheres are widely used in the pharmaceuticals, biomaterials, and modern chemical industry. Montejoa *et al.* develops a batch of microspheres *via* single-emulsion (O/W) solvent evaporation method.[20] They investigate the influences of molecular weights on the morphology, size distributions, and biocompatibility of resultant microspheres. Studies find that such novel and convenience method have a potential application in sustained drug release. Genchi *et al.* fabricates an injectable moxidectin sustained release (SR) formulation with PLGA microspheres as carriers for preventing the infection of canine heartworm.[21] A single injection of moxidectin SR formulation administered *via* subcutaneous injection at 0.17 mg/kg (0.05 mL/kg of reconstituted suspension) is effective to prevent heartworm infection in the dog bodies for the full season. Amoozgar *et al.* prepares novel PLGA-based nanoparticles to deliver paclitaxel.[22] Such nanoparticles achieve a 3.8-fold higher loading content compared to that of nanoparticles obtained from linear PLGA-PEG copolymers. Such nanoparticles can be used to formulate injections, which decrease the systemic toxicity of paclitaxel and improve their therapeutic effects. In addition, the nanoparticles may have higher efficacy but trigger low toxic reactions. However, such technology is too complicate to be applied in industrial manufacture. W. Sheng *et al.* uses hydrogel as the carriers of avermectins to prolong their insecticidal effects.[23]

Nevertheless, due to the property of hydrogel, such formulation can only be administrated *via* oral method instead of injection. Therefore, the pesticide effect can not last for a long time. S. Rehbein *et al.* investigates the efficacy of EPR extended-release injection (ERI) against infections with third-stage larvae or eggs of gastrointestinal and pulmonary nematodes in cattle.[24] Though the extended-release effect of ERI is detailedly investigated, the fabrication process of ERI is not described. T. Chen *et al.* prepares a batch of novel PLGA microspheres *via* a solvent evaporation method, and the *in vitro* release behavior of EPR from EPR-loaded microspheres is also studied.[25] The convenient technology can effectively produce the EPR-loaded microspheres industrially on a large scale. The medicated microspheres exhibit extend-release behaviors, but the *in vivo* release profiles are not mentioned in their investigations. M. D. Soll *et al.* develops a batch of EPR extended-release injections with PLGA microspheres as carriers. They investigate the *in vivo* release profile of this formulation, and study find that the formulation can provide high levels of parasite control against a range of nematodes of cattle for up to 5 months following a single injection.[26] However, the allergization of injection on the administrated site is not mentioned in their lecture. Recent years, though many lectures report EPR-loaded PLGA microspheres as sustained-release injections, many of them are focus on the persistent efficiency of their formulations. The fabrication processes of microspheres are seldom introduced in detail, and investigation of the sensitization on injection site is absent.

In this study, the mesoporous PLGA microspheres were fabricated *via* a syringe

pump, and such technology was firstly introduced in the extend-release of pesticides. The biggest advantage of such method is that microspheres sizes were easily to be controlled by adjusting the flow rates of PLGA solutions. EPR was employed as a model drug, and encapsulated into such mesoporous microspheres to fabricate a sustained-release injection. Then, Japanese White rabbit were employed in the monitor of EPR plasma concentrations. In rabbit bodies, those EPR loaded in the macropores of PLGA microspheres would release first, which endowed such injection a quick-acting effect. Subsequently, the EPR trapped in microspheres were diffused out gradually, which ensures the formulation with a persistent effect. Similar *in vivo* release profile of EPR was not reported in previous lectures. Besides, we firstly studied the sensitization response of such formulation on the injected skins, which provided fundamental basis for improving the compatibility of EPR injection.

## 2. Experimental section

### 2.1 Materials

EPR was purchased from Hebei Veyong Bio-Chemical Co. Ltd. PLGA (50:50 lactic acid: glycolic acid) were received from Lakeshore Biomaterials. Poly (vinyl alcohol) (PVA-1788) with an alcoholysis degree of 88 % and an average polymerization degree of  $1750 \pm 50$  was supplied by Sigma-Aldrich (USA). Dichloromethane (DCM) and ethyl acetate (EA) were obtained from Sigma-Aldrich (USA). EPR injection was the product of Hebei Veyong Bio-Chemical Co. Ltd. Methanol and acetonitrile with

HPLC grade were from Damao Chemical Co., Ltd (Tianjin, China). Other chemicals were of reagent grade and used directly without any further treatment.

## 2.2 Microspheres preparation

The EPR-loaded microspheres were obtained *via* an emulsion-solvent evaporation method.[27] Briefly, accurately weighed PLGA was dissolved into the organic solvents (DCM or EA) to obtain PLGA solutions with the concentrations of 40.0 mg/mL. Subsequently, certain amounts of EPR were added into above solutions under magnetic stirring to gain homogeneous solutions (70.0 mg/mL). The final solution was loaded into a 5.0 mL syringe equipped with a 26G blunt-end-needle (inter diameter 0.4 mm). Under violent magnetic stirring (1, 200 r/min), above solution was delivered into a 2.0 wt% PVA aqueous solution with a 74900-05 syringe pump (Cole-Parmer, USA) at the speed of 0.5 mL/h. For solvents evaporation, the final microspheres suspension was stirred for another 5 h under ambient temperature. The resultant microspheres were recovered by lyophilization from an LGJ-10 freezing drier (Beijing, China). Then, 1.0 mL of mannitol aqueous solutions (20.0 W/V%) was added into the microspheres to prevent them from aggregation. The lyophilized microspheres were stored in a vacuum desiccator for further study.

## 2.3 Morphology

The surface morphology of microspheres was observed *via* SEM (Hitachi S-4800, Japan). Prior to observation, specimens were fixed onto the specimen disc with conducting resin. To render them electrically conductive, all specimens were platinum

coated under argon atmosphere, and their morphology was observed with a field emission gun operated at 3.0 kV.

#### 2.4 FTIR

To confirm the hydrogen bonds between EPR molecules and PLGA matrix, the FTIR (BIO-RAD FTS-135, USA) study were carried out. Specimens of EPR, blank microspheres, and EPR-loaded microspheres were prepared in KBr pellets under a hydraulic pressure of 400.0 kg. The infrared spectra were obtained from an FTIR spectrophotometer and recorded in the adsorption mode from 3500 to 500  $\text{cm}^{-1}$ .

#### 2.5 Distribution states of EPR

DSC analysis was performed to study the thermal performances of EPR in microsphere with a calorimeter (DSC 200F3 Netzsch, Germany). Accurately weighed samples (approximately 10.0 mg) were put into aluminium pans. Under the protection of nitrogen gas ( $\text{N}_2$ ), the pans were heated from 0 °C to 200 °C at the heating rate of 10 °C/min. To intuitively observe the crystal structures of EPR in microspheres, the XRD curves of original EPR, blank microspheres, EPM, and EPR/PLGA composites were carried out using an XRD-700 X-ray crystal diffractometer (Shimadzu, Japan). The scans were recorded at room temperature with  $2\theta$  ranging from 0 to 60°. The specific crystal data were obtained from a Jade 6.0 software.

#### 2.6 *In vitro* drug release studies

Accurately weighed 35.0 mg of EPR-loaded PLGA microspheres were filled into a dialysis bag (cut off molecular weight 1, 000 Da) pretreated with 2.0 mL phosphate

Buffer solution (PBS, pH 7.4). The system was kept in a beaker flask pretreated with 28.0 mL PBS containing 0.02 w/v% sodium azide to interfere with the growth of bacteria. All flasks were incubated in a ZHWY-100H circulating water oscillator (ZHICHENG analytical instrument manufacturing, China) under 37 °C, and all flasks were oscillated at a speed of 70 rpm. At predetermined intervals, 1.0 mL of PBS was withdrawn from flasks, and replenished with same volume of fresh PBS. After filtrating with 0.45 µm filtration membrane, the EPR concentrations were determined by high performance liquid chromatography (HPLC) in triplicate.[28] A *t*-test analysis was carried out, and data were considered significant difference at  $p < 0.05$ .

The concentration of EPR was detected by HPLC (Waters, e2695) with a reversed phase C18 column (4.6 mm × 150 mm-5 µm, Hypersil ODS2) at the wavelength of 245 nm. The column was fixed in a column oven to keep the temperature at 25 °C. A mixture of acetonitrile, water, and trifluoroacetic acid (75/25/0.01, v/v/v) was employed as the mobile phase, and the flow rate was set as 1.0 mL/min. Each experiment was repeated 3 times, and the results were expressed as mean value ± S.D. The drug-loading and encapsulation efficiency (EE) of microspheres was calculated with following Equations:

$$\text{Drug - loading} = \frac{\text{weight of drugs loaded in microspheres}}{\text{weight of microspheres}} \times 100\% \dots \dots \dots (1)$$

$$\text{EE} = \frac{\text{measured drug loading}}{\text{theoretical drug loading}} \times 100 \% \dots \dots \dots (2)$$

## 2.7 Plasma concentrations

Japanese white rabbits were employed in plasma concentrations studies after

acclimatizing for 7 days. Prior to subcutaneous injection, all rabbits were allowed access to drinking water ad libitum but fasting overnight. Then, all rabbits were injected 0.15 mg/kg (5.0 mg/mL) of EPM suspension in a randomized order. The weight of each rabbit was measured and recorded before subcutaneous injection. 0.15 mL plasma specimen was collected in dried heparinized tubes at appropriate intervals after subcutaneous injection. 100.0  $\mu$ L of plasma sample was transferred into a 2.0 mL eppendorf tubes, and then, 250.0  $\mu$ L of anhydrous methanol was added to above plasma samples. Then, the mixture was centrifuged at 3000 rpm for 10.0 min in microcentrifuge. The supernate was transferred into another tube, and the EPR concentrations in blood were determined with HPLC method in triplicate.

## 2.8 Biocompatibility

Kunming mice (20.0-30.0 g, 8 weeks) were employed for *in vivo* evaluation the biocompatibility of microspheres. Before evaluation, microspheres were sterilized *via*  $^{60}\text{Co}$ - $\gamma$  radiation. To avoid the pyrogen reactions, ultrapure water were applied to disperse the lyophilized microspheres, and the concentration of obtained suspension solution was 25.0 wt%. Then, 0.4 mL of above suspension was injected into the backs of Kunming mice (0.4 mL). For comparison purposes, mice in control group were injected 0.4 mL normal saline and EPR injections (Hebei Veyong Bio-Chemical Co. Ltd) under the similar conditions. The weight of individual mouse was measured before their scheduled sacrifice on the 1<sup>st</sup>, 3<sup>rd</sup> and 7<sup>th</sup> day after subcutaneous injection. After necropsy, skin tissues at injection sites were extracted and immersed in Bouin's solution for 7 days. After washing with ultrapure water, skin specimens were cut into

slices with the thickness of 2.0 mm. Subsequently, all skin specimens were dehydrated in alcohol (chromatographic grade) and embedded in paraffin. The transverse sections with the thickness of 4.0-5.0  $\mu\text{m}$  were prepared using rotatory microtome. Before histopathological examination, all specimens were stained with hematoxylin and eosin dye. Histological changes in injection sites, such as: acute-chronic inflammatory symptoms, leukocytosis, fibroblastic proliferation and any other inflammatory responses, were observed under an Eclipse E200 optical microscopy (Nikon, Japan).

All the Kunming mice used in experiments were fed in individual cages in controlled environments with free access to water and food. Animal experiments were carried out in accordance with the People's Republic of China National Standard (GB/T 16886.6-1997).

### **3. Results and discussion**

#### **3.1 Fabrication of PLGA microspheres**

DCM is the most commonly solvent used in the fabrication of microspheres. Its good solubility for various polymers makes it convenient to control the properties of final microspheres. EA, as a non-chlorinated solvent, is considered as another excellent solvent from the viewpoint of environment, human safety and product approval.[29] Therefore, DCM and EA were selected as solvents in the fabrication of EPR-loaded microspheres in this study. The morphology of different microspheres prepared with both solvents was shown in Fig. 1. Microspheres obtained from DCM were in

spherical shapes, and many macropores were observed on their surfaces (Fig. 1 a and b). Statistic studies showed that the macropores had a size distribution of  $747.8 \pm 260.0$  nm. The formation of macropores might be due to the rapid evaporation of DCM and the fast solidification of final microspheres. During this process, crust firstly formed on the surface of PLGA solution droplets with DCM evaporation. However, these crusts blocked the further evaporation of DCM entrapped in PLGA solution droplets.[30] For effectively reducing the inner pressure, many macropores formed on the crust (shown in Figure S1). By contrast, microspheres prepared from EA were spherical with uniform size distribution (Fig. 1d), but no macropores were observed on the surface of these microspheres (Fig. 1e). This phenomenon could be explained by the relatively higher boiling point (BP) and residual of EA. The higher BP and residual of EA resulted in a lower inner pressure, which could not induce the forming of macropores. Therefore, DCM used as solvent to prepared mesoporous microspheres, while EA was applied in the fabrication of microspheres (without macropores).

### 3.2 EE of microspheres

With the same drug-loading, the EE of EPM was slightly lower than that of EPR-loaded PLGA microspheres (EM, microspheres without macropores), but the difference between both kinds of microspheres was not obvious. This phenomenon might be due to the relatively high water solubility of EA (7.0-8.0 wt%) but low hydrophilicity of EPR (6.0-9.0  $\mu\text{g/L}$ ). When EA was used as a solvent, EPR was hard to be extracted into the aqueous phase during the process of microsphere hardening.

Therefore, much EPR was encapsulated into the final microspheres. On the contrary, the quick evaporation of DCM might lead EPR to leak out from the microspheres. Hence, a relative smaller drug-loading was observed in EPM. Similar phenomena had been reported in the encapsulation of meloxicam.[31] However, the slightly high water solubility of EA might result in forming non-spherical (collapsed or deflated) microspheres with EA evaporation.[32]

### 3.3 Distribution states

Drug crystals in formulations always destroy the solubility and bioavailability of model drugs. To avoid these disadvantages, crystalline drug usually distributed in vehicles with the amorphous states. The states of model drugs in formulations were detected using DSC and XRD methods. DSC technique could provide qualitative information about the thermal properties of crystalline drugs during their melting process. Therefore, the DSC curves could indirectly reflect the distribution states of model drugs in carriers.[33] On the contrary, XRD curves could intuitively reflect the crystal textures of crystalline drug.[34]

DSC analysis of as-received EPR, original microspheres, the mixture of EPR and microspheres, and EPM was carried out and shown in Fig. 2. The sharp endothermic peak exhibited at 171.2 °C was corresponding to the melting point ( $T_m$ ) of EPR. In Fig. 2c, the endothermic peak at 45.9 °C was the glass-transition temperature ( $T_g$ ) of PLGA. In the DSC curves of EPM, only the  $T_g$  of PLGA was observed but the  $T_m$  of EPR (171.2 °C) disappeared. These changes indicated that EPR existed in the microspheres with an amorphous state. On the contrary, a melting peak of EPR was

observed in the DSC curves of the EPR/PLGA mixture, which suggested that crystalline EPR distributed in the mixture. These data illustrated that the EPR-loaded microspheres could inhibit EPR from separating crystal out, and the encapsulated EPR was in an amorphous state.

XRD patterns of all specimens were carried out and shown in Fig. 3. EPR was a crystalline drug for many diffraction peaks were observed on the XRD pattern of EPR at the  $2\theta$  of  $5.7^\circ$ ,  $7.2^\circ$ ,  $11.3^\circ$ ,  $13.1^\circ$ , and  $17.1^\circ$ . The broad peak in the XRD pattern of blank PLGA microspheres was the typical endothermic peak of PLGA. Excepting the diffraction peak of PLGA, no diffraction peaks of EPR ( $2\theta$  of  $5.7^\circ$ ,  $7.2^\circ$ ,  $11.3^\circ$ ,  $13.1^\circ$ , and  $17.1^\circ$ ) was observed in the pattern of EPM. These results illustrated that PLGA microspheres inhibited EPR re-crystallization, and these data were according with the DSC results.

The medicated microspheres inhibited EPR from re-crystallization, which could be explained by two main reasons. Firstly, the solidification process “frozen” EPR in the microspheres, which decreased the mobility of EPR molecules and inhibited EPR from re-crystallization to a certain degree. Secondly, the hydrogen bonds would increase the compatibility between EPR molecules and microsphere matrix. To confirm the forming of hydrogen bonds, FTIR spectra of as-received EPR, blank PLGA microspheres and EPM were carried out (shown in Fig. 4). The adsorption peaks observed at approximately  $3357.6\text{ cm}^{-1}$  in the spectrum of as-received EPR was due to the stretching vibration of  $-\text{OH}$  groups (Fig. 4a). In the spectrum of EPM, the adsorption peak shifted to the lower wave-number area ( $3318.79\text{ cm}^{-1}$ , Fig. 4b). In Fig.

4b, the band observed at  $1736.74\text{ cm}^{-1}$  was due to the vibration of carbonyl groups of PLGA matrix, which also showed a blue-shift phenomenon ( $1733.98\text{ cm}^{-1}$ ) in Fig. 4c. These changes indicated that new hydrogen bonds generated between the  $-\text{OH}$  groups in EPR and the carbonyl groups in PLGA matrix.

### 3.4 *In vitro* release study

In the release study, 40.0 % anhydrous alcohol was added into PBS (v/v) to maintain the “sink condition” in release studies. The sizes of microspheres had great effects on the *in vitro* releasing profiles of EPR. Under the circumstances, the influences of microspheres sizes on the release behaviors of EPR were studied (Fig.5). It could be seen from Fig.5 that three release profiles were approximate S-curves, but the release rates of EPR were different. EPM with the diameter range of 20-50  $\mu\text{m}$  showed the fastest release behavior. In the 17<sup>th</sup> day, release profile reached to its equilibrium state with the maximum EPR amount of  $91.56 \pm 2.67\%$ . However, with the diameters growing, the equilibrium times were also prolonged. EPM with the diameters of 75-100  $\mu\text{m}$  needed 26 day to reach the release equilibrium ( $95.34 \pm 4.56\%$ ), while these EPM with the diameters of 100-150  $\mu\text{m}$  reached to the release equilibrium state in the 35<sup>th</sup> day ( $95.43 \pm 1.49\%$ ). It could be seen that EPM with the diameter range of 100-150  $\mu\text{m}$  showed the longest release time. Therefore, EPM with the diameter range of 100-150  $\mu\text{m}$  was employed for further releasing studies.

The release difference between EPM and EM were carried out with the EPR/PLGA composite as a control, and the results were depicted in Fig.6. It could be seen that  $98.76 \pm 2.31\%$  of EPR was released from the EPR/PLGA composite in the 1<sup>st</sup> day.

This phenomenon indicated that the EPR/PLGA composite did not show a sustained release effect. The burst release of EPR/PLGA composite would result in the fluctuation of blood concentrations, or even triggered toxic effects to laboratory animals. By contrast, EPR was slowly and continuously released from EPM and EM suspensions, and this process lasted over 40 days. The EPR release rate from EPM was relatively larger than that from EM. In the first 5 days,  $11.58 \pm 2.34$  % of EPR released from EPM, while only  $2.37 \pm 0.48$  % EPR diffused from EM. After 29 days' releasing, approximately  $93.50 \pm 0.67$  % EPR was diffused from EPM, but only  $73.87 \pm 5.30$  % was released from EM. A *t*-test showed the differentials between both groups of releasing data were significant ( $p < 0.05$ ).

The difference was mainly due to the different structures of both kinds of microspheres. The good compatibility between EPR and microspheres made EM release EPR at a slow and constant rate. In EPM, EPR was trapped in the macropores and inside of microspheres (Fig. 7). During the release process, EPR trapped in macropores would release quickly, which ensured EPM with a fast-acting effect. Subsequently, the EPR loaded inside of microspheres would be diffused into PBS, gradually. Therefore, such release profile endowed EPR with a quick-acting and persistent effect.

### 3.5 Plasma concentrations

Dried EPM and EM were re-dispersed in ultrapure water to obtain suspension solutions with a concentration of 5.0 mg/mL. Both microspheres suspensions were used in the monitoring of plasma concentrations, and the EPR injection (Hebei

Veyong Bio-Chemical Co. Ltd, Hebei) was employed as a control. After subcutaneous injection, the plasma concentration-time profiles of EPM, EM, and EPR injection were carried out (Fig. 8). It could be seen that the plasma concentrations of EPR injection was fluctuant. The  $C_{max}$  of  $51.60 \pm 5.05$  ng/mL was observed at the 1<sup>st</sup> day of injection. Even worse, EPR could not be detected in the blood samples in the 20<sup>th</sup> day of injection, which illustrated that the purchased EPR injection did not showed a sustained-release effect. However, EPM profile exhibited a  $C_{max}$  of  $38.80 \pm 9.50$  ng/mL at the  $T_{max}$  of 2 days after subcutaneous injection. In the next 40 days, the plasma concentrations of EPR were maintained at 30.0 ng/mL, which illustrated that the EPM suspension had a persistent effect. By contrast, the blood concentration of EM suspension was maintained at 20.0 ng/mL during the whole monitoring period. The EM suspension also showed a sustained-release effect, but its plasma concentration was smaller than that of EPM suspension. Therefore, EPM and EM suspensions showed sustained-release effects, but EPM suspension had better quick-acting and persistent effects than those of EM suspension.

Four groups of Balb/c mice were used to study their survival rates after the subcutaneous injection. Mice in Group A (control) were administrated with 0.1 mL normal saline *via* subcutaneous injection. Groups B were injected 0.1 mL blank microspheres suspension. Group C were injected 0.1 mL EPM suspension (containing 0.1 mg EPR), and group D were administrated 0.5 mL EPR injection (containing 0.1 mg EPR). The survival rates of all mice was depicted in Fig. 9. During the experimental period, no sacrifice was observed in Group A, which illustrated that the

normal saline was safe to mice. In Groups B, first death happened after 9 days of injection, and another mouse died in the 25<sup>th</sup> day. The survival rate of mice in Group B was 80.0%. In Group C, three mice died in the 5<sup>th</sup>, 17<sup>th</sup>, and 36<sup>th</sup> day, respectively, and the survival rate of Group C was 70.0%. By contrast, in Group D, two mice died in the 5<sup>th</sup> and 27<sup>th</sup> day, respectively. In general, the survival rate of mice in four groups was 100.0 %, 80.0 %, 70.0 % and 80.0 %, respectively. After *t*-test analysis, there were no significant differences between four groups ( $p>0.05$ ). These data indicated that the microspheres suspension were safe for subcutaneous injection.

### 3.6 Evaluation of biocompatibility

The irritation of EPM suspension to the mice skins of injection sites were carried out for consecutive 7 days. Fig. 10 exhibited the representative histopathological changes extracted from the injection sites. After one day of subcutaneous injection, inflammatory response was observed at the injection sites by the increased permeability of capillaries and infusion of abundant lymphocytes. In the next day, the inflammation response increased for many lymphocytes and neutrocytes were observed (Fig. 10a). Nevertheless, new fibroblast cells generated around the injection sites after 3 days of injection (Fig. 10b). After 7 days, a new and thin fibrous tissue formed under the dermal layer and superficial layer of the muscularis, and the histology was similar to that of normal skin (Fig. 10c). During the experimental period, tissue samples showed an indication of time-related healing process. However, no significant histological differences were observed between control (Fig. 10d-f) and EPM suspension samples. Thus, histopathological studies suggested that EPM was

biocompatible for subcutaneous injection.

#### 4. Conclusions

The mesoporous PLGA microspheres were fabricated *via* an emulsion (O/W) solvent evaporation method. The XRD and DSC data indicated that EPR distributed in microspheres with an amorphous state. *In vitro* release studies showed that EPM exhibited a fast and constant release profile. Japanese white rabbits were administrated by subcutaneous injection, and the peak plasma concentration ( $C_{max}$ ) was appeared at the 2<sup>nd</sup> day after injection. In the next 40 days, the plasma concentrations were maintained at around 30.0 ng/mL. These phenomena illustrated that EPM had a fast-acting and persistent effect. In addition, EPM did not trigger serious stimulus response at the injection sites. Therefore, the mesoporous microspheres had a promising application in sustained release of veterinary drug.

**Acknowledgements** This work was financed by the Natural Science Foundation of Hebei province, China (No. C2011208111).

## References

1. V. Cozma, E. Suteu, C. Gherman, B. Losson, *Sci. Parasitol.* 2010; 11, 105-107.
2. H. Q. Wen, B. L. Pan, Y. W. Wang, *Vet. Parasitol.* 2010; 174, 72-76.
3. S. Rehbein, J. E. Holste, L. L. Smith, J. L. Lloyd, *Vet Parasitol.* 2013; 1, 192, 353-358.
4. M. Kh. Dzhafarov, S. Yu. Zaitsev, M. N. Mirzaev, D. N. Urazaev, V. I. Maksimov, *Russian Agricultural Sci.*, 2010, 36, 130-132.
5. R. B. Davey, J. A. Miller, J. E. George, J. A. Klavons, *J. Med. Entomol.*, 2007; 44, 277-282.
6. F. A. Borges, H. C. Silva, C. Buzzulini, V. E. Soares, E. Santos, G. P. Oliveira, A. J. Costa, *Vet. Parasitol.* 2008; 155, 299-307.
7. J. Dupuy, J. F. Sutra, M. Alvinerie, L. Rinaldi, V. Veneziano, L. Mezzino, S. Pennacchio, G. Cringoli, *Vet. Parasitol.* 2008; 157, 284-290.
8. R. B. Davey, J. M. Pound, J. A. Miller, J. A. Klavons, *Vet. Parasitol.* 2010; 169, 149-156.
9. A. Gossner, H. Wilkie, A. Joshi, J. Hopkins, *Vet Res.* 2013; 44, 68.
10. M. Reist, A. B. Forbes, M. Bonfanti, W. Beretta, K. Pfister, *Italy Vet. Rec.* 2011; 168, 484-487.
11. M. R. Virto, B. Elorza, S. Torrado, M. L. Elorza, G. Frutos, *Biomaterials.* 2007;

- 28, 877-885.
12. X. H. Ren, S. C. Liu, J. W. Dai, F. Hou, L. G. Zhou, T. G. Lv, *Livest Sci.* 2011; 137, 124-129.
  13. F. J. Byrne, A. A. Urena, L. J. Robinson, R. I. Krieger, J. Doccola, J.G Morse, *Pest Manag. Sci.*, 2012; 68, 811-817.
  14. Z. H. Hu, Y. J. Liu, W. E. Yuan, *Colloid Surface B.* 2011; 86, 206-211.
  15. F. Sun, C. Sui, L. Teng, X. Liu, L. Teng, Q. Meng, Y. Li, *Int. J. Pharm.* 2010; 397, 44-49.
  16. X. Chen, L. Wang, Q. Liu, J. Jia, Y. Liu, W. Zhang, G. Ma, Z. Su, *Int. Immunopharmacol.* 2014; 23, 592-602.
  17. A. P. Griset, J. Walpole, R. Liu, A. Gaffey, Y. L. Colson, and M. W. Grinstaff, *J. Am. Chem. Soc.* 2009; 131, 2469-2471.
  18. W. Sheng, S. Ma, W. Li, Z. Liu, X. Guo, X. Jia. *RSC Adv.*, 2015; 5, 13867-13870.
  19. Y. Yan, H. Hou, T. Ren, Y. Xu, Q. Wang, W. Xu. *Colloids Surf. B. Biointerfaces.* 2013; 1, 341-347.
  20. C. Montejoa, E. Barciab, S. Negrob, et al., *Int. J. Pharma.*, 2010; 387, 223-229.
  21. M. Genchi, G. Pengo, C. Genchi, *Vet Parasitol.* 2010; 28, 170, 167-169.
  22. Z Amoozgar, L Wang, T Brandstoetter, S. S. Wallis, E. M. Wilson, M. S. Goldberg, *Biomacromolecules*, 2014; 15, 4187-4194.

23. W. Sheng, S. Ma, W. Li, Z. Liu, X. Guoac X. Jia, RSC Adv. 2015; 5, 13867-13870.
24. S. Rehbein, D. G. Baggott, E. G. Johnson, B. N. Kunkle, T. A. Yazwinski, S. Yoon, L. G. Cramer, M. D. Soll, Vet Parasitol. 2013, 1, 192, 321-331.
25. T. Chen, Y. Y. Liang, Y. G. Zhao, X. Y. Zhang, T. S. Qi, Q. Shang, Adv. Mater. Res. 2014; 936, 746-750.
26. M. D. Soll, B. N. Kunkle, G. C. Royer, T. A. Yazwinski, D. G. Baggott, T. A. Wehner, S. Yoon, L. G. Cramer, S. Rehbein. Vet Parasitol. 2013; 1, 192, 313-320.
27. D. Gilmore, Y. L. Colson, Semin Thorac Cardiovasc Surg. 2011; 23, 10-11.
28. Y. Sun, J. C. Wang, X. J. Zhang, J. Control. Release. 2008; 129, 41-48.
29. Z. Hao, J. Wuhan. Univ. Technol. 2013; 28, 1242-1245.
30. Q. Shang, X. Wang, M. Apley, S. B. Kukanich, C. Berkland, J. Vet. Pharmacol. Ther. 2012; 35, 231-238.
31. D. Gilmore, M. Schulz, R. Liu, K. A. Zubris, R. F. Padera, P. J. Catalano, M. W. Grinstaff, Y. L. Colson, Ann. Surg. Oncol. 2013; 20, 1684-1693.
32. J. A. Camargo, A. Sapin, D. Daloz, P. Maincent, J. Microencapsul. 2010; 27, 609-617.
33. R. Nanda, A. Sasmal, P. L. Nayak, Carbohydr. Polym. 2011; 83, 988-994.
34. Y. Shi, S Xu, A. Dong, J. Zhang, J. Mater Sci-Mater. M. 2013; 24, 333-341.

## Tables

**Table. 1** Effects of solvents on the EE of PLGA microspheres

Drug-loading rate (%)	EE (%) <sup>a</sup>	
	DCM	EA
10.0	93.8 ± 1.5	92.4 ± 1.8
15.0	92.4 ± 1.8	91.8 ± 1.4
20.0	91.8 ± 1.4	92.4 ± 1.8
25.0	91.3 ± 1.1	92.1 ± 1.8

<sup>a</sup> The data in table is the average of three determination and standard deviation

## Figure captions

**Fig. 1** Morphology of different EPR-loaded microspheres fabricated from various solvents. a) Microspheres prepared with DCM as a solvent (EPM); b) Surface morphology of EPM; c) Microspheres prepared with EA as a solvent (EM); and d) Surface morphology of EM.

**Fig. 2** DSC thermograms of various specimens. As-received EPR showed a melting point at about 171.0 °C, but the endothermic peak disappeared from the DSC curve of EPR-loaded microspheres. This phenomenon illustrated that EPR distributed in PLGA microspheres in an amorphous state.

**Fig. 3** XRD patterns of different testing specimens. a) as-received EPR, b) original microspheres, c) the mixture of EPR and microspheres, and d) EPM. As-received EPR was crystalline for many diffraction peaks were observed in its XRD pattern. However, these crystal structures of EPR were not observed in EPM. These changes also confirmed that EPR was loaded in microspheres in an amorphous state.

**Fig. 4** FTIR spectra of as-received EPR (a), blank PLGA microspheres (b), and EPM (c). In FTIR spectra, the bands attributing to -OH groups of EPR molecules and carbonyl groups of PLGA matrix shifted to the lower wave-number areas, which indicated new hydrogen bonds generated from EPR molecules and PLGA matrix.

**Fig. 5** Release profiles of EPR from different EPR-loaded microspheres with various sphere sizes.

**Fig. 6** *In vitro* release profiles of EPR from EPM, EM and EPR/PLGA composite suspensions. Due to a part of EPR distributed in macropores, EPM showed a fast and

constant EPR release behavior.

**Fig. 7** Release mechanism of EPR from EPM. EPR was loaded in the macropores and inside of microspheres. With the protection of mannitol, a preservative was generated on the surface of microsphere, which blocked EPR to diffuse under dry state. When EPM suspended in water, the preservative was destroyed and EPR trapped in macropores released firstly. Subsequently, EPR loaded inside of microspheres would diffuse into PBS continuously.

**Fig. 8** Whole plasma concentration-time profiles of EPR after injection 0.15 mg/kg of EPR, 5.7 mg/kg of EPM suspension (0.15 mg/kg of EPR), and 5.7 mg/kg of EM suspension (0.15 mg/kg of EPR). Each point represented the mean  $\pm$  S.D. (n = 6).

**Fig. 9** Kaplan-Meier survival curves of four groups of administrated Balb/c mice. These mice were administrated by injection of normal saline (control), blank microspheres suspension, EPM suspension (containing 0.1 mg EPR), and EPR suspension (containing 0.1 mg EPR) (each group containing 10 Balb/c mice).

**Fig. 10** Representative histopathological changes noted at the injection sites of EPM on the 1st (a), 3rd (b) and 7th days (c); Histopathological changes observed at the injection sites of normal saline on the 1st (e), 3rd (f) and 7th days (g) (100, N: Neutrocyte; CF: Collagenous fiber; FT: Fibrous tissues).

Fig. 1

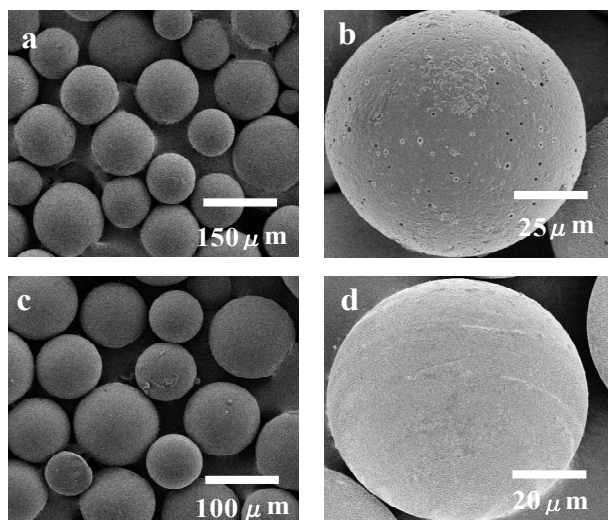


Fig. 2

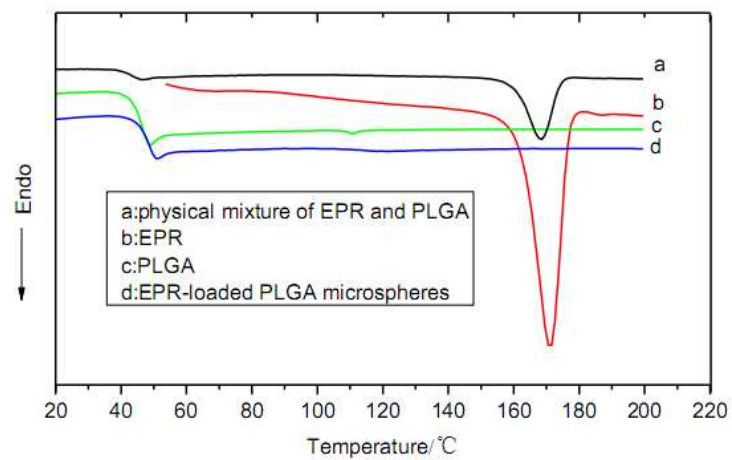


Fig. 3

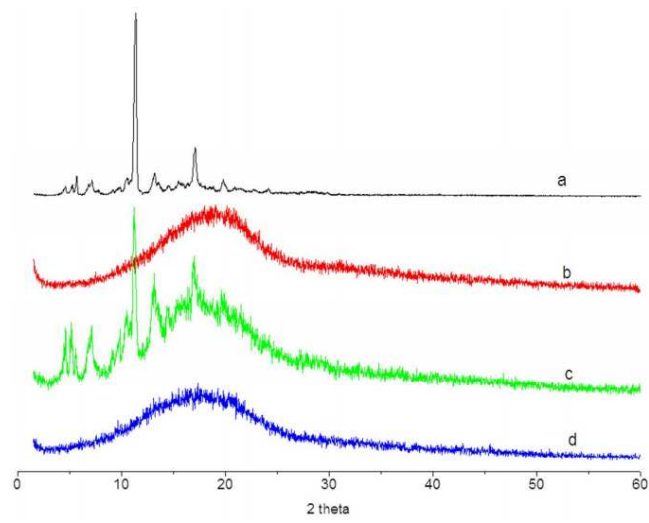


Fig. 4

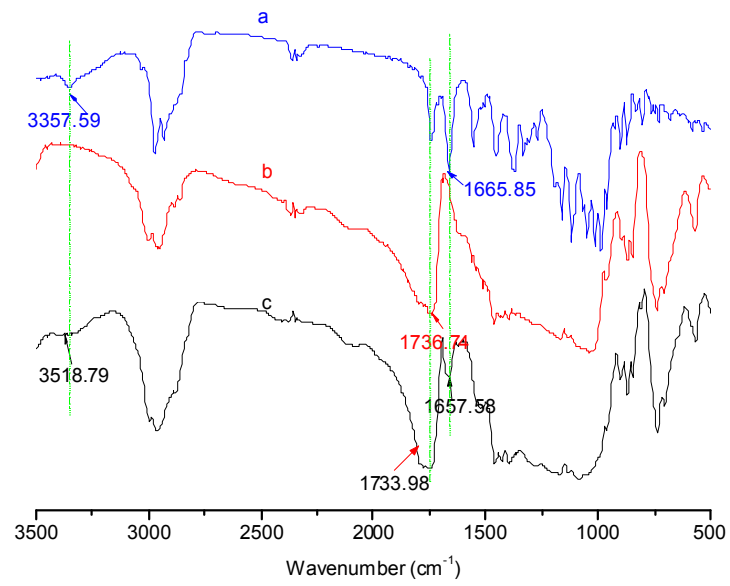


Fig. 5

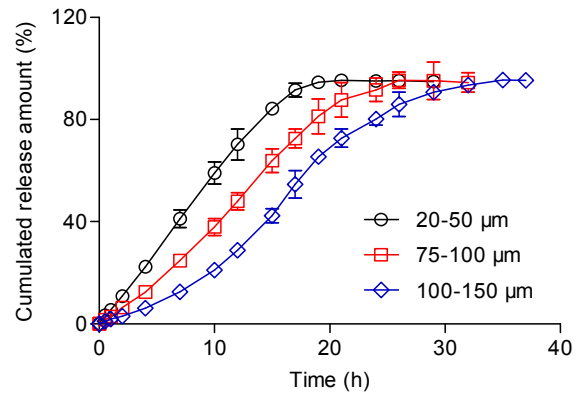


Fig. 6

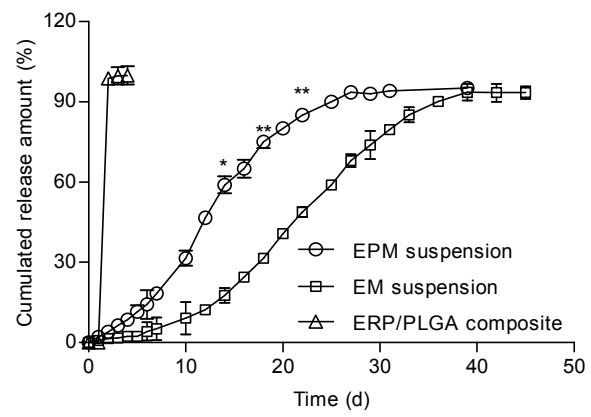


Fig. 7

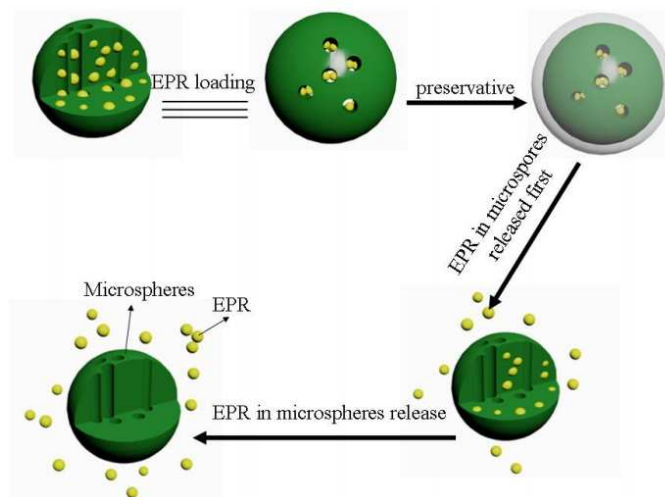


Fig. 8

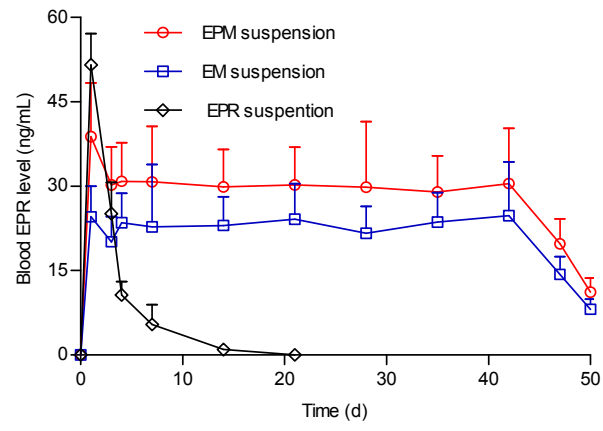


Fig. 9

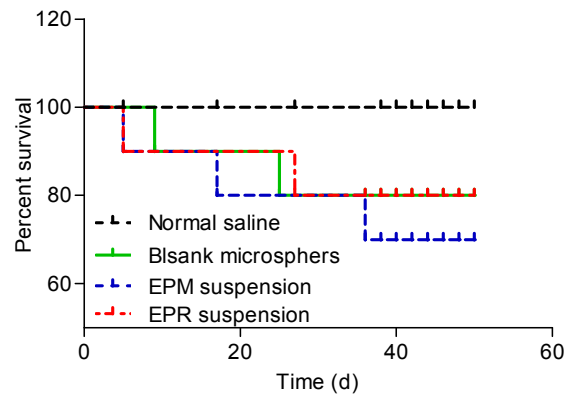


Fig. 10

